Hindawi
International Journal of Geophysics
Volume 2022, Article ID 7588306, 22 pages
https://doi.org/10.1155/2022/7588306

Research Article

Multichannel Analysis of Surface Waves (MASW) to Estimate the Shear Wave Velocity for Engineering Characterization of Soils at Hawassa Town, Southern Ethiopia

Alemayehu Ayele,[1,2] **Kifle Woldearegay**,[3] **and Matebie Meten**[1]

[1]*Department of Geology, College of Applied Sciences, Addis Ababa Science and Technology University, Addis Ababa, P.O Box 16417, Ethiopia*
[2]*Department of Geology, College of Natural and Computational Science, Wachemo University, Hosanna, P.O Box 667, Ethiopia*
[3]*School of Earth Sciences, Mekelle University, Mekelle, P.O Box 231, Ethiopia*

Correspondence should be addressed to Alemayehu Ayele; alex98geo@gmail.com

Received 27 July 2022; Revised 27 November 2022; Accepted 30 November 2022; Published 19 December 2022

Academic Editor: Salvatore Gambino

Site characterization is a prerequisite for the successful and economic design of engineering structures and earthworks by providing geological information for any proposed project. Until now, no detail study has been carried out on the site characterization and classification using shear wave velocity (Vs) up to the top 30 m depth in Hawassa town. For this study, multichannel analysis of surface waves (MASW) was used to determine the variation of Vs for a proper civil engineering design in the town. In addition, vertical electrical sounding (VES) and standard penetration test (SPT) were employed to characterize the near-surface materials. The Vs30 map was prepared for Hawassa town using the estimated Vs30 values which ranges from 248.9 m/s to 371.3 m/s while the SPT-N values were ranges from 5bpf to 50bpf. The correlation of Vs and SPT-N values has been done by considering both corrected and uncorrected SPT-N values. The VES result showed that groundwater is found at a shallow depth. The correlation of Vs and SPT-N value was validated using regression model. The 1D Vs profile and 2D cross-section showed low Vs at a shallow depth. The near-surface soils of the town are classified based on the Vs30 as site class C (stiff soil and soft rock) and D class (stiff soils) according to the NEHRP (Natural Earthquake hazards Reduction Program) and as subsoil classes B and C according to the Eurocode 8. The geotechnical tests also showed that the soils in the study area are silty sand, sand and silty sand with some gravel. The low Vs values observed at a shallow depth should be given much attention during foundation design for the stability of civil engineering structures.

1. Introduction

Population growth, rapid urbanization, and the demand of new land for infrastructures expansion of many Ethiopian cities including Hawassa town requires providing the necessary information about an existing soil condition, elastic moduli, bedrock depth, ground stiffness, site class and groundwater table for the safe design, construction, and its long service. Insufficient or inadequate soil characterization leads to unsatisfactory design which may subsequently result in serious structural damage or failure. Therefore, a detail geophysical and geotechnical site characterization plays an important role to identify a suitable site for any proposed structures and thus to prevent the engineering structures and human life from any future unexpected catastrophic consequences [1, 2].

Civil engineering structures in Hawassa town are constructed with no detailed information of the subsoil characterization which acts as the basic foundation material that support and stabilize the any engineering structures [3, 4]. Structural failure is usually linked to the use of substandard materials and poor investigation of the subsoil materials. The main reason for structural failure emanates from inadequate understanding on geophysical and geotechnical properties of a soil. Moreover, the nature/type of soils, geologic

sequence, and structures and water bearing units also affect the stability of civil engineering structures. These properties provide reliable information to effectively characterize the heterogeneous subsoil beneath an engineering site so as to construct successful structure [5, 6]. Buildings, roads, bridges, and high ways are infrastructures that contribute significantly to the sustainable development of the town. Therefore, it is necessary to have an adequate plan for a proper construction of the superstructure for a long time service and minimize an economic loss [7]. A detail understanding on the type, nature and characteristics of the soil, geological structures, depth of a groundwater table, and competent bedrock is most valuable to geotechnical and earthquake engineers for a proper site selection, design of an engineering structures, and identification of the possible adverse and unfavorable conditions in the study area in order to adopt proper remedial measures [8, 9].

Several studies have used integrated geophysical and geotechnical investigations to characterize its suitability of the near-surface materials for road, building constructions, and foundation [10–13]. On this regards, multichannel analysis of surface waves (MASW) are widely used to measure the shear wave velocity (Vs) of near-surface materials as these methods are reliable, noninvasive, and low-cost procedures in engineering applications to identify potentially unsuitable geological conditions, determine small-strain stiffness of soil and rock, foundation instability analysis, and know site classes [14–16]. Rayleigh waves that propagate from the ground surface to subsurface are used to estimate Vs from the dispersion curve and thus the average shear wave velocity (Vs30) is estimated from the measured Vs to determine the site class for site response analysis, earthquake resistant design and safe building provision [17, 18]. It is also an important geotechnical parameter to obtain the near-surface dynamic properties of a soil which in turn is essential for the engineering design of a small to large projects such as roads, buildings, and highways. The vertical electrical sounding (VES) is proven to be very efficient and applicable technique in groundwater investigation, landfill site, and engineering site characterization and foundation stability analysis [19, 20]. This is particularly applied to engineering site investigation as it measures the resistivity variation within the near-surface as a function of factors like grain size distribution, soil structure and stratification, and degree of water saturation. Therefore, this helps to decide on the suitability of the site for the effective design of structural foundations and sustainable building constructions.

Due to its simplicity, the standard penetration test (SPT) is the most widely used dynamic in-situ test in geotechnical site investigation for describing the dynamic properties of a soil in foundation stability analysis [21]. Many researchers have used SPT-N values to identify the stiffness of a soil, depth of groundwater table, soil profile/type, site class, and relative density as these are very important to assure the suitability of a site for a building foundation [22–24]. Different researchers have been correlated Vs and SPT-N values to check the degree of relationship between these parameters [25–28]. In the current study, the detail soil properties and type, site classes, stiffness, elastic moduli, and correlation of Vs and SPT-N values, competent bedrock depth, layer boundaries, and depth of water table has been studied with in a view of engineering site characterization to ensure the suitability of a site for any civil engineering structure [29, 30]. The main aim of this study was investigating the near surface geological materials in Hawassa town using MASW, VES, and SPT survey and thus determines whether the study area is suitable for a safeguard construction and indestructible infrastructure development in the future. This can be done by identifying the soil type and stiffness, estimating Vs30, and providing site class for the selecting a proper foundation.

2. Location and Geological Setting of the Study Area

The town of Hawassa is situated in the southern Main Ethiopian Rift (MER) at the center of Hawassa caldera, on the eastern and southeastern sides of Lake Hawassa (Figure 1). The study area is geographically bounded between longitude 7°1′ to 7°5′N and latitude 38°28′ to 38°29′E. The MER is an active plate boundary between the Nubian and Somalian plates which controls the seismic activity in the East African region [31]. The seismicity in and around Hawassa town includes earthquakes of minor to intermediate magnitudes (M <6) that have caused structural damage to buildings and infrastructures in the town [32–35]. In addition, this town is located in the shade of two silicic volcanoes that have emerged from the floor of the middle Pleistocene Corbetti Caldera [36]. According to [36] the lithological units in Hawassa town and its environs include fluvial sediments, alluvial sediments, polygenetic sediments, Wondo Koshe pumice fall and flow deposits, scoria cones, tuff cones, Hawassa basalts, and Hawassa rhyolitic ignimbrites (Figure 2).

3. Materials and Methods

3.1. Geotechnical and Borehole Data. SPT approach was applied to determine soil stiffness, thickness, and depth of the near-surface materials [37, 38]. For this purpose, forty one SPT borehole data were collected from private organizations for the site characterization, correlation of Vs and SPT-N values, and seismic site classification [39, 40] (Figure 3). All the collected SPT-N data was corrected using the correction factor as stated in Table 1 for hammer efficiency, borehole diameter, rod length, and sampler liner [41, 42] according to equation (1). Then, the obtained N60 was used for the correlation with Vs. Laboratory tests were conducted, including grain size analysis, moisture content, and Atterberg limits, on selected soil samples to determine the geotechnical properties and to identify the soil type/properties and grain sizes of each soil according to the specification of [43] of soils in the study area.

$$\mathrm{N60} = \frac{\mathrm{EH} * \mathrm{CB} * \mathrm{CS} * \mathrm{CR} * \mathrm{SPT} - \mathrm{N}}{0.6}. \quad (1)$$

where N60 is the corrected SPT-N value in the field, EH is the hammer efficiency, CB is the borehole diameter, CS is the sampling method, CR is the rod length and SPT-N is the

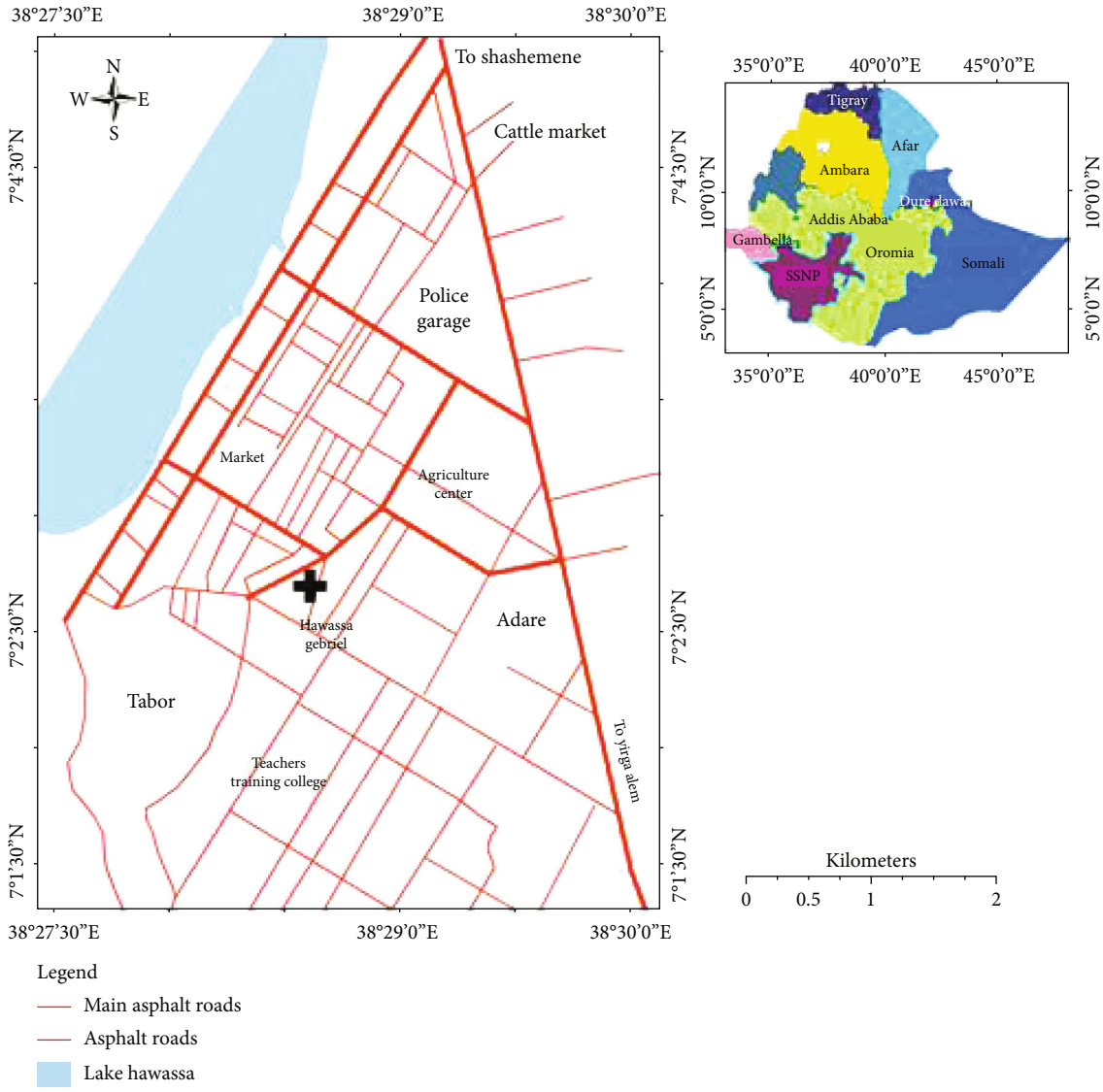

Figure 1: Location map of Hawassa town in Southern Ethiopia.

measured value in the field. Forty borehole data was obtained from the south design construction and construction supervision enterprise (Figure 4) [44]. This information was used to prepare the borehole distribution and groundwater level maps in the study area using ArcGIS.

3.2. Geophysical Data Acquisition

3.2.1. MASW Data Acquisition. Nineteen MASW data points at 5 m spacing were used for data acquisition on the study area (Figure 3). MASW data sites were selected based on the accessibility of a site to spread the geophones. To measure the Vs, MASW measurements were carried out across the investigated sites (Figure 4) using Geode seismograph instrument. This system consists of 24 geophone channels (4.5HZ). Surface waves were generated by striking a metal plate which is tightly coupled to the ground surface by a 10 kg sledge hammer. The number of impacts (i.e. stacks) at each shooting point was 5 to increase the signal-to-noise ratio and thus improve the data quality. MASW data acquisition parameters were employed in the present study is listed in Table 2.

3.2.2. VES Data Acquisition. In the current study area, two VES surveys were conducted for this investigation using ABEM Terrameter SAS 300C Resistivity Meter (Figure 4). Four electrodes (two current electrode and two potential electrodes) were used in this study to make a contact to the ground. The Schlumberger array/configuration was used for VES data collection by 150 m current electrode spacing (AB/2) according to the accessibility of a site for measurement. On the other hand, the potential electrode (MN) spacing starts from 0.5 m to 45 m were used to investigate the near-surface earth materials. Each VES points contain 16 apparent resistivity measurements. For the two VES surveys, the measured apparent resistivity values were plotted against the AB/2 on a log-log scale to control the consistency of values in the study area.

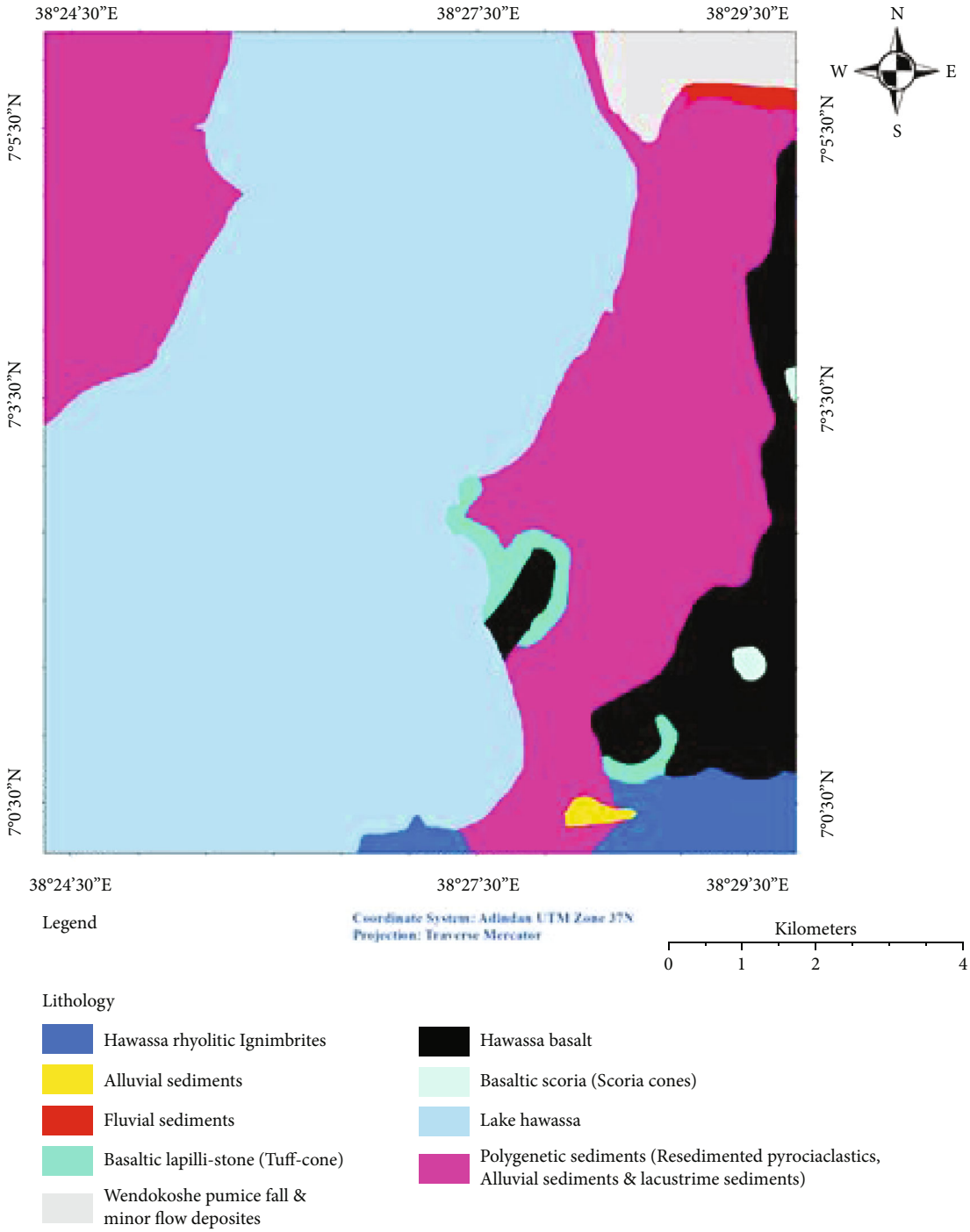

Figure 2: Geological map of Hawassa area (modified after [36]).

3.3. Data Processing

3.3.1. MASW. Based on the geological conditions of the study area, five representative sites of MASW data points were selected for the detail analysis. The shot gathers acquired during the MASW were analyzed using SeisImager/SW software to obtain the dispersion curves, 1D and 2D Vs cross-section of the investigated area. The cross correlation of common midpoint (CMP) gather was applied to generate the dispersion curve at the frequency domain. The Vs were calculated from the phase velocity versus frequency curve using the phase velocity dispersion curve. The linear slope of each component on the swept frequency record was used to compute the phase velocity. The spatial variation of Vs with depth was observed in the 1D Vs profile whereas the spatial variation of Vs with depth versus distance was seen in the 2D Vs cross section in the investigated area.

Figure 3: Data acquisition using Geode seismograph instrument in the field.

Table 1: Correction factors used in the field to determine SPT-N values in this study [41].

Factors	Terms	Equipment variable	Correction factor
Hammer efficiency	EH	Donut hammer	0.5
Borehole diameter	CB	65–155 m	1
Sampling method	CS	Standard sampler	1
Rod length	CR	3–4 m	0.75
		4–6 m	0.85
		6–10 m	0.95
		>10 m	1.00

3.3.2. VES. In order to estimate the layer parameters (layer thickness and true resistivity) in the study area, the IP2WIN [45] inversion software was used. The main steps followed in this study to determine the layer thickness and true resistivity were inputting the field data, fitting the measured, and calculated curves and invert these curves. More number of iterations was used to get the best fit for the measured and calculated resistivity curves. The final model was used to interpret and relate with the geological conditions of the study area.

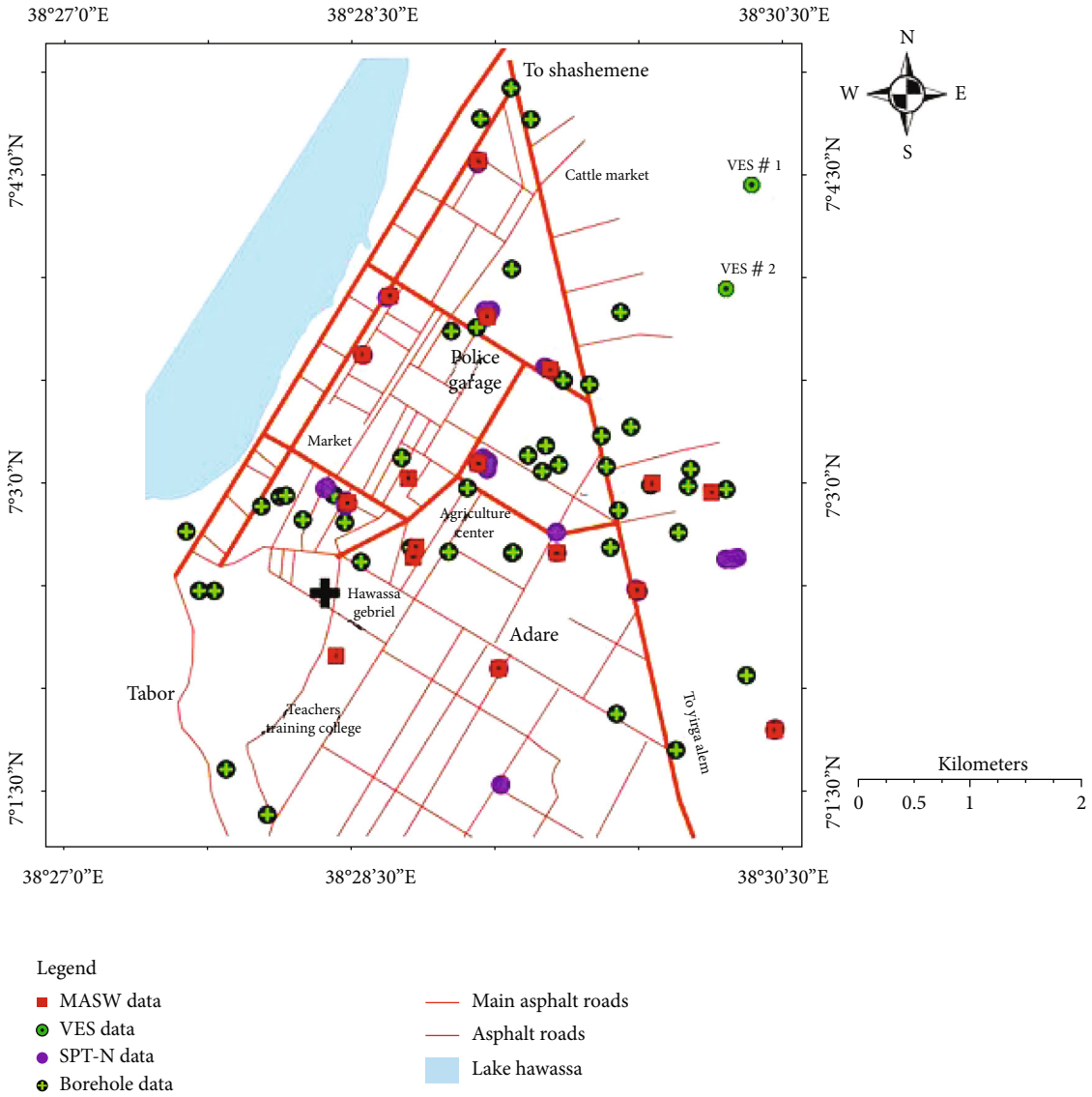

Figure 4: Location of boreholes, SPT-N, MASW, and VES data points in Hawassa town.

4. Vs30, Shear Modulus (G30max) and Modulus of Elasticity (E30) Calculations

Vs profiles, which are obtained by inverting Rayleigh wave dispersion curves, are used to determine Vs30 [46]. Vs30 values were calculated in this study using [47, 48]

$$V_{s30} = \frac{30}{\sum_{i=0}^{N} (di/Vi)}, \quad (2)$$

where di and vi denote the thickness (in meters) and shear wave velocity of the ith formation or layer, respectively, from a total of N layers in the top 30 m. The empirical link between P-wave velocities (Vp) and Vs was used to estimate Vp of the porous/saturated materials in the investigated area. The Vp of saturated materials is 1500 m/s by [49] but these values range between 1200 m/s and 1800 m/s according to [50, 51]. To estimate Vp, the measured Vs was used according to [52].

$$V_p = 1.11 * V_s + 1290, \quad (3)$$

where Vp is the compressional wave velocity which can be estimated from the measured Vs and Vs is the shear wave velocity measured from the field using MASW. The Gmax and E30 estimated from the measured Vs was used to characterize the investigated site [53]. For this purpose, G30max and E30 which are given in equation (4) [54] and 5 [55], respectively, were used to characterize the soil condition of the sites in the study area.

$$G30\ \max = \rho(Vs30)^2, \quad (4)$$

Table 2: MASW data acquisition parameters.

Energy/source	Sledge hammer
Geophone	24 geophones of 4.5 Hz frequency
Stack	5
Geophone distance	5 m
Length of spread	115 m
Shot position	Every 5 m interval (starting from -2.5 m to 117.5 m)
Recoding time	2000 ms
Sampling	0.125 ms
Filter	Open

Table 3: Existing empirical correlations between Vs and SPT-N values employed for this investigation depending on the soil type from the other experts.

S.no	Authors	Vs (m/sec) Sandy soils
1	Shibata [58]	$Vs = 32(SPT - N)^{0.5}$
2	Ohta et al. [59]	$Vs = 87.2(SPT - N)^{0.36}$
3	Imai [60]	$Vs = 80.6(SPT - N)^{0.331}$
4	Imai and Tonouchi [61]	$Vs = 97(SPT - N)^{0.314}$
5	Seed et al. [62]	$Vs = 56.4\,(SPT - N)^{0.5}$
6	Sykora and Stokoe [63]	$Vs = 100.5\,(SPT - N)^{0.29}$
7	Lee [64]	$Vs = 57.4(SPT - N)^{0.49}$
8	Hasançebi and Ulusay [65]	$Vs = 90.82(SPT - N)^{0.319}$
9	Hanumantharao and Ramana [66]	$Vs = 79(SPT - N)^{0.434}$
10	Dikmen [67]	$Vs = 73(SPT - N)^{0.33}$
11	Rahman [68]	$Vs = 82(SPT - N)^{0.3829}$
12	This study	$Vs = 115(SPT - N)^{0.28}$

where G30max is the average shear modulus (Pa) in the top of 30 depth and Vs30 is the average shear wave velocity (m/s) up to a depth of 30 m and ρ is the average density of the soil (in kg/m^3).

$$E30 = 2(V_s30)^2[\rho + \sigma], \tag{5}$$

where E30 is the average modulus of elasticity (Pa) at a depth of 30 m, Vs30 is the average shear wave velocity (m/s) in the top of 30 m depth, and σ is Poisson ratio and a standard value of 0.25 was used [56].

5. Correlation of Vs and SPT-N

The correlation between Vs and SPT-N value was used for an engineering site characterization [57]. Table 3 shows the statistical links between Vs and SPT-N values proposed by the several researchers for this purpose. They also looked at empirical power-law relationships between Vs and SPT-N values like $Vs = A(SPT - N)^B$, where A controls the amplitude of Vs and the SPT-N value curve, B controls the relationship curvature, Vs is the shear wave velocity, and SPT-N represents the standard penetration test values as shown in Table 3. The Vs values were predicted from the SPT-N values using a regression relationship for sandy soil in this study, and it was compared to other available empirical equation around the world.

The validation of the regression equation for the predicted Vs and measured Vs values is required to ensure the model produced for the study area is reliable. Researchers employed the normal consistency ratio (Cd) and comparison between predicted and measured Vs to validate the predicted Vs [69, 70]. The predicted Vs were validated using a Cd and comparison of measured Vs in this investigation. Cd is also calculated using equation (6) [67] as the ratio of the difference between the Vspre and Vsmeas divided by SPT-N values

$$Cd = \frac{(Vsmeas - Vspred)}{SPT - N\,values}, \tag{6}$$

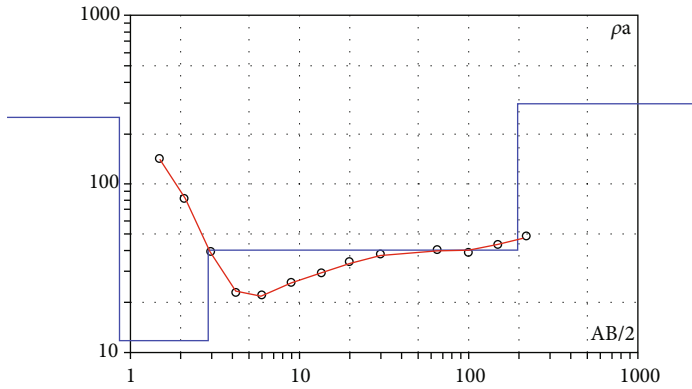

N	ρ	h	d	Alt
1	250	0.847	0.847	−0.8471
2	11.7	2	2.85	−2.849
3	40.2	192	195	−194.6
4	303			

(a)

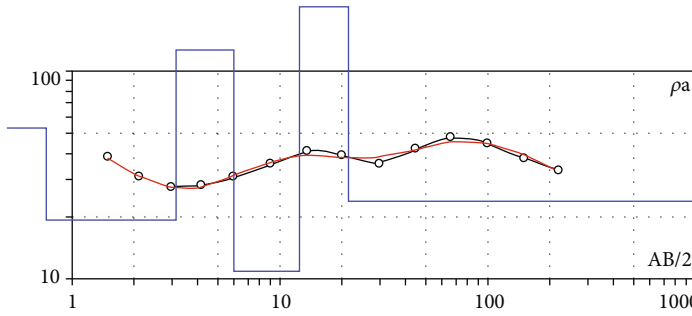

N	ρ	h	d	Alt
1	53.5	0.75	0.75	−0.75
2	19.3	2.43	3.18	−3.177
3	126	2.82	6	−6
4	10.9	6.32	12.3	−12.32
5	274	9.06	21.4	−21.39
6	23.5			

(b)

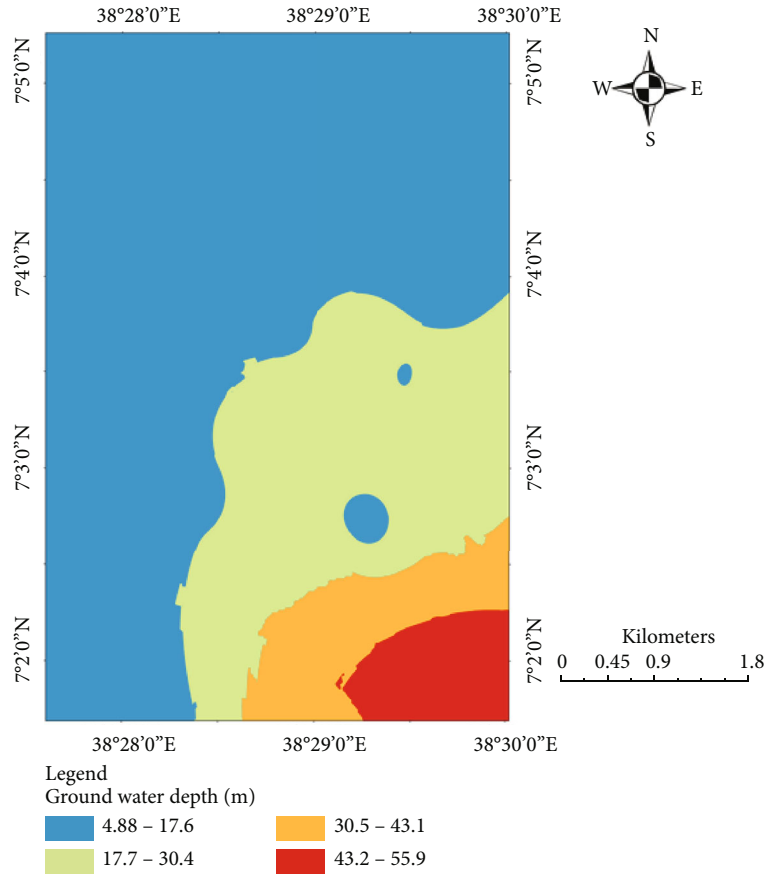

(c)

Figure 5: (a) VES1 inverted ρ graph, (b) VES2 inverted ρ graph, and (c) groundwater level map from the borehole in Hawassa town.

where Vsmeas is the measured shear wave velocity, Vspred is the calculated Vs using the newly proposed regression equation for the study area, and SPT-N values are the measured SPT-N values.

6. Results and Discussion

6.1. VES. The resistivity models created by inverting the VES data revealed differences in resistivity (ρ) with depth in the investigated area. In Figure 5(a), the VES1 showed HA type curve ($\rho 1 > \rho 2 < \rho 3 < \rho 4$) with an acceptable RMS error of 1.83 percent. There are four geo-electrical layers. As shown in Table 4, the first layer has a high ρ layer (250 ohm-m at a depth of 0.847 m), the second layer has a very low ρ layer (11.7 ohm-m at a depth of 2.85 m), which is considered a shallow aquifer, the third layer has a low ρ layer (40.2 ohm-m at a depth of 195 m), and the fourth layer has a very high ρ layer (303ohm-m). As illustrated in Figure 5(b), the inverted VES2 revealed HKK type curve ($\rho 1 > \rho 2 < \rho 3 > \rho 4 < \rho 5 > \rho 6$). In total, there are six geo-electrical strata in which the first layer exhibits a high ρ zone (53.5 ohm-m at 0.75 m), whereas the second layer depicts a low ρ layer (19.3 ohm-m at 3.18 m), which is probably interpreted as a shallow aquifer. The third layer has a very high ρ (126 ohm-m at a depth of 6 m), the fourth layer has a very low ρ (10.9 ohm-m at a depth of 12.3 meters), the fifth layer has an ρ increase (27.4 ohm-m at a depth of 21.4 m), and the sixth layer has shown a decrease in ρ (23.5 ohm-m). The study has shown similar trends with that of [71]. The spatial analysis of borehole data in Hawassa town showed that the groundwater level ranges from 4.88 m to 55.9 m. As shown in Figure 5(c), the groundwater level in the northwestern and southwestern parts of the study area is shallower than that of the southeastern part (see the Supplementary Table S1 and Figure S1). The groundwater level in Hawassa town is generally shallow and increases in its depth from the western to the eastern parts of the town. The VES and borehole data points were taken from different sites in the study area as shown in Figure 4. However, the VES data showed that groundwater table probably found at a shallower depth than from the borehole data.

6.2. 1D Vs Profiles and 2D Vs Cross-Section. The findings from five sites (MASW 1, MASW 2, MASW 3, MASW 4, and MASW 5) were provided in this study. The RMS is less than 7% and thus it was acceptable. The Vs models in Figure 6 showed that the typical sites have Vs values range from 168 m/s to 542 m/s whereas Vp values which were estimated from the measured Vs values ranging from 1477 m/s to 1892 m/s (Supplementary Table S2 and Figure S2). Vp was estimated from Vs values. Vs and Vp values exhibited significant depth variability for three sites (MASW 1, MASW 2, and MASW 5): (a) a decrease in value was observed in the upper layer (0 to 5 m) which indicated lithological variation; (b) an increase in value was observed in the depth range of 5 m to 25 m; and (c) a decrease and nearly constant values were observed at depths greater than 25 m. However, because of lithological alterations, the

Table 4: Thickness (h) and resistivity (ρ) of VES 1 and VES 2 at Hawassa town.

VES 1			VES 2		
Layer	Depth (m)	Resistivity (Ω m)	Layer	Depth (m)	Resistivity (Ω m)
h1	0.847	250	h1	0.75	53.9
h2	2.85	11.7	h2	3.18	19.3
h3	195	40.2	h3	6	126
		303	h4	12.3	10.9
			h5	21.4	27.4
					23.5

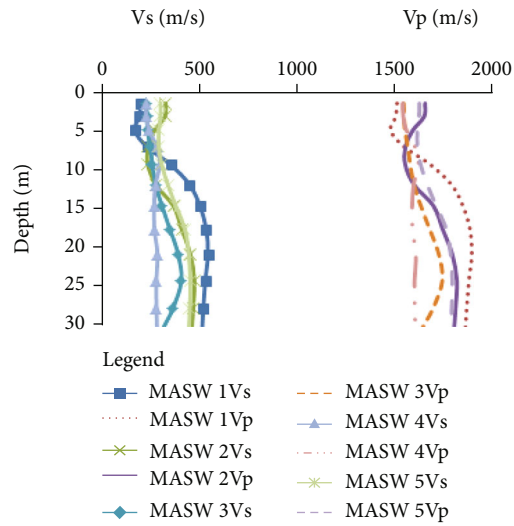

Figure 6: Vs and Vp plots for typical sites in the study area.

Vs and Vp values of MASW 3 decreased from 0 to 25 m before start it starts to drop or remain constant from 25 m onwards. The top layer (depth 0 to 5 m) of MASW 4 showed a drop in Vs and Vp values, indicating lithological variation, although the value remained constant at depths greater than 5 m. The dispersion curve in (Figure 7(a)) was constructed at a frequency of 5.4 Hz to 19 Hz and a phase velocity from 200 m/s to 450 m/s. Due to weak overtone image, the dispersion curve at a frequency below 5.4 Hz was not shown for MASW 1 (Figure 7(a)) but the dispersion curves at a frequency below 5.2 Hz were not shown for MASW 2, MASW 3, MASW 4, and MASW 5 (Figures 7(b)–7(e)). The dispersion curves were showed at a frequency interval of 5.2 Hz to 19 Hz for selected sites in the study area but the phase velocity for the selected sites were range from 200 m/s to 450 m/s. The phase velocity and frequency curves revealed a smooth curve that begins high on the left and then drops low on the right for MASW 1, MASW 2, MASW 3, and MASW 5 (Figures 7(a)–7(c) and 7(e)) but phase velocity and frequency curves showed almost straight line for MASW 4.

The Vs values vary from 191 m/s to 542 m/s for 1D Vs profile for MASW 1 (Figure 8(a)). The data revealed that a

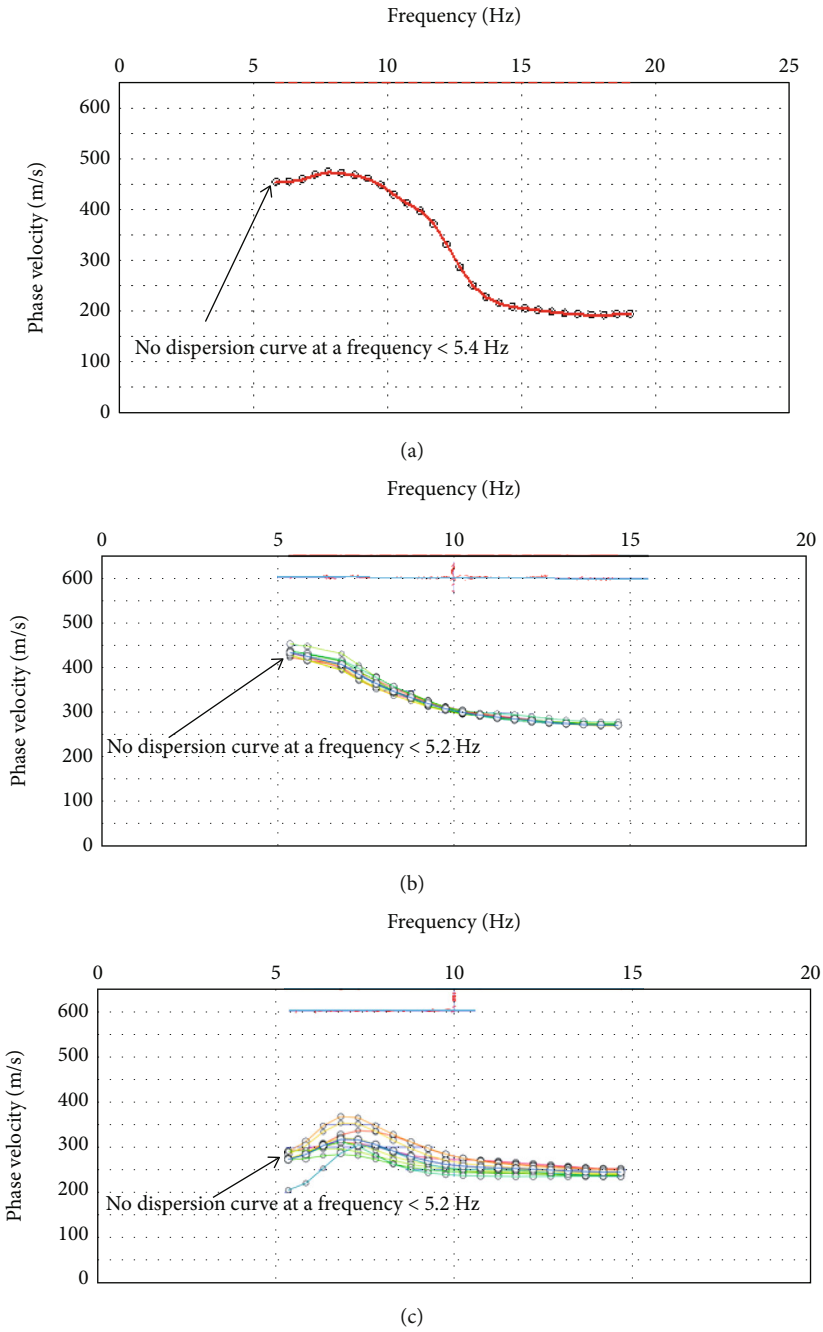

Figure 7: Continued.

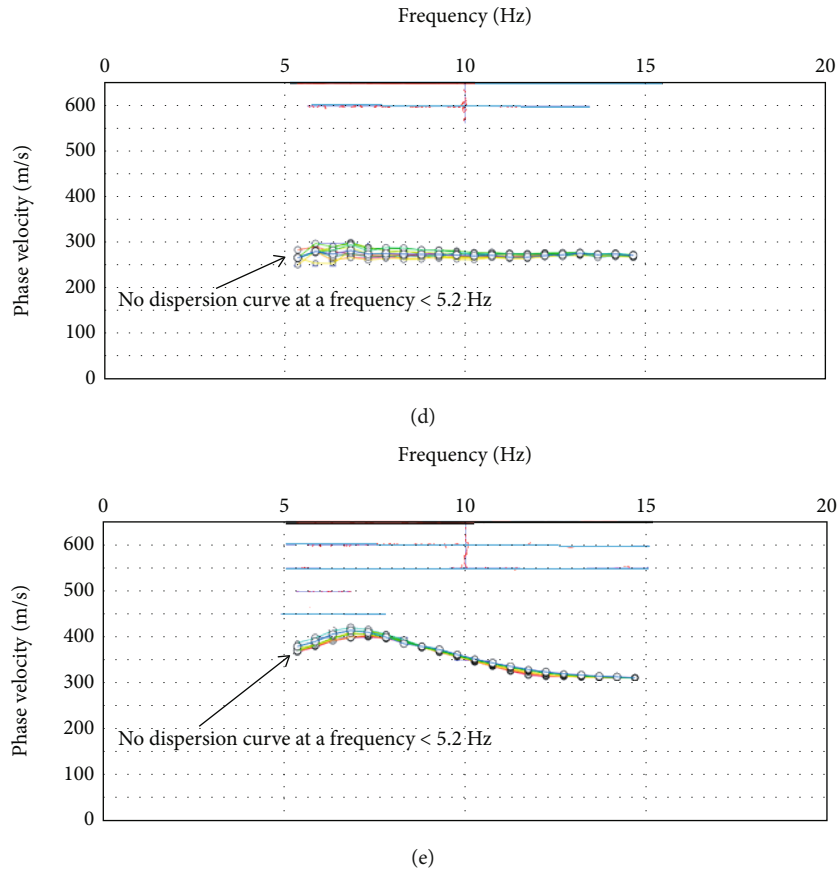

Figure 7: Dispersion curves from (a) MASW 1, (b) MASW 2, (c) MASW 3, (d) MASW 4, and (e) MASW 5.

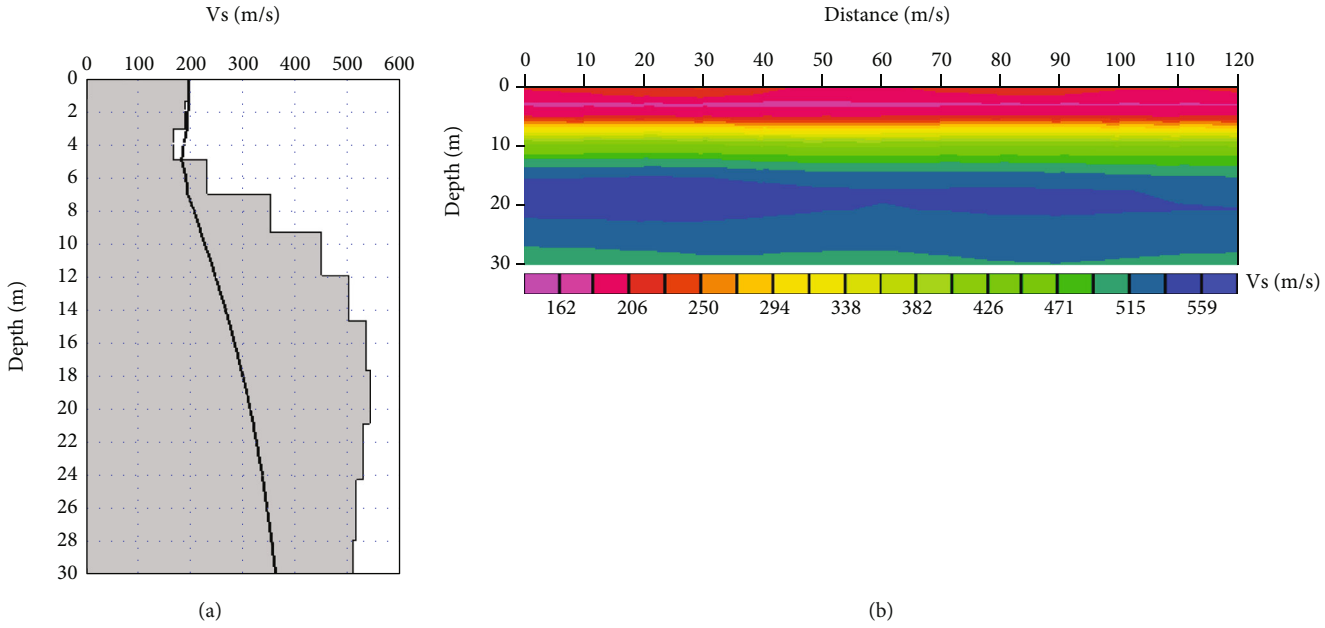

Figure 8: (a) MASW 1 1D profile and (b) 2D Vs cross-section.

rise from 200 m/s at the surface to 542 m/s at a depth of 0 and 20 m, respectively, and then it drops from 540 m/s to 501 m/s at a depth of 20.8 m and 30 m, respectively, due to its lithological variation. As it was observed in Figure 8(b), the 2D Vs cross-section of MASW 1 showed Vs variation at a lateral distance of 120 m. In addition, it

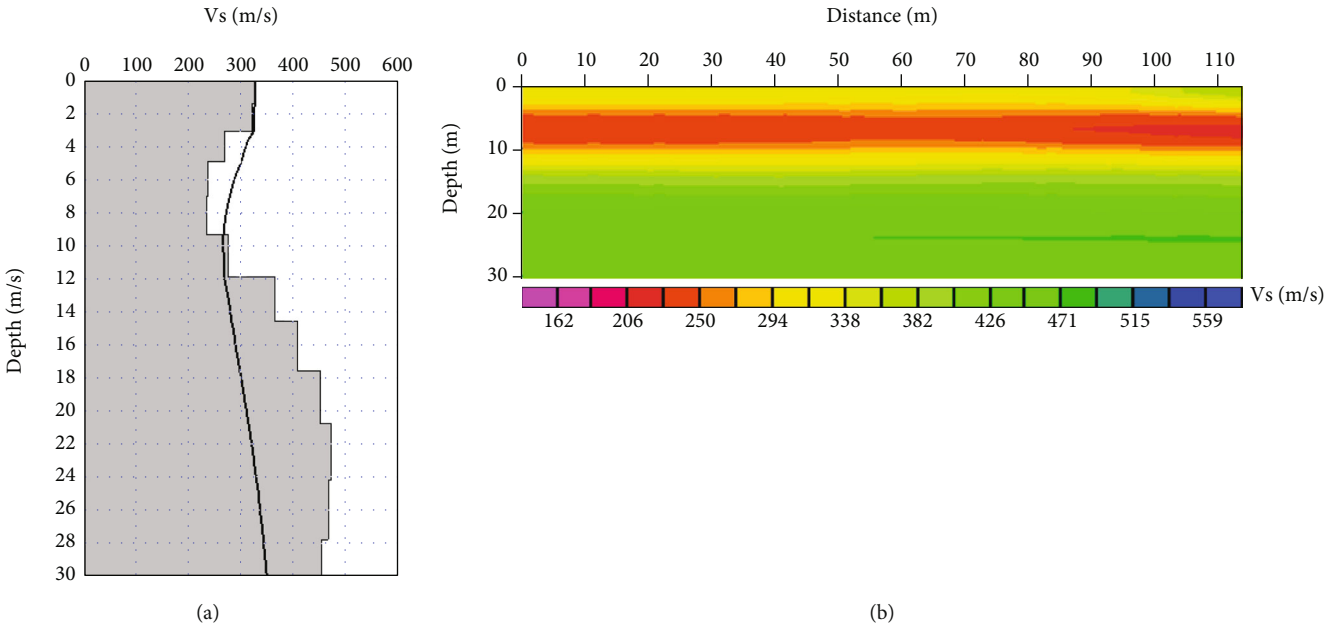

Figure 9: (a) MASW 2 1D profile and (b) 2D Vs cross-section.

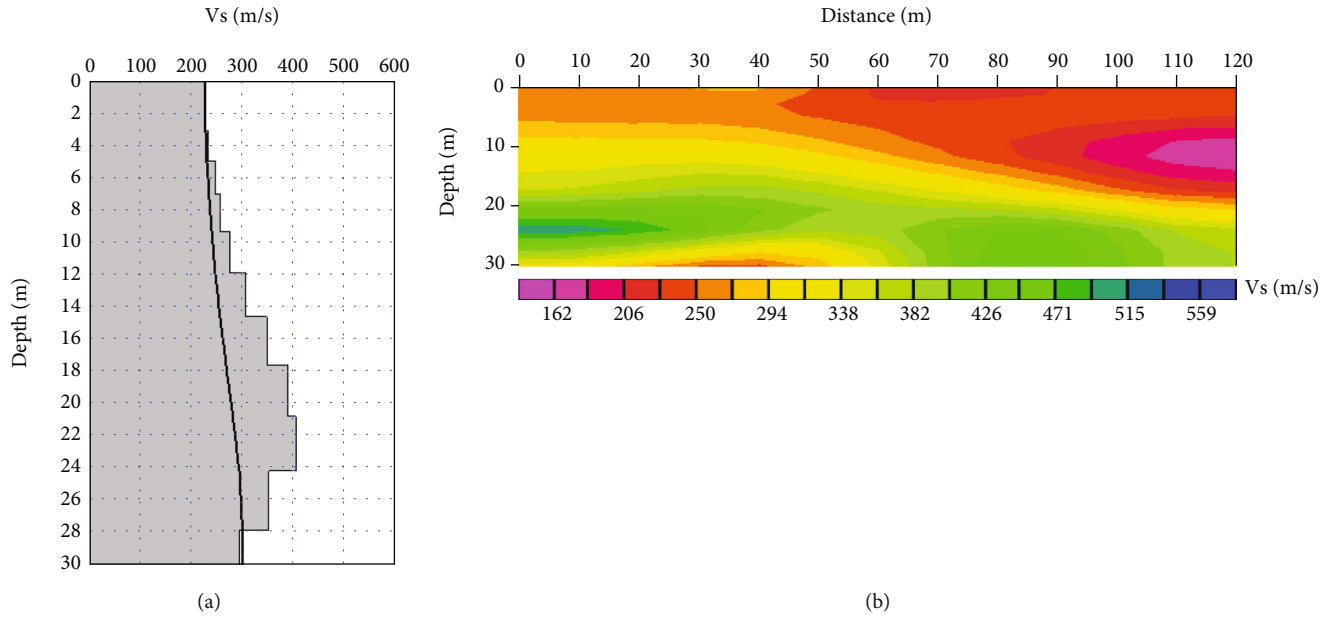

Figure 10: (a) MASW 3 1D Vs profile and (b) MASW 2D vs cross-section.

showed a low Vs values between 0 to 5 m, a very high Vs contrast between 12 m and 25 m which is most probably caused by the response of stiff materials. There was also a slight decrease in Vs values at a depth of 30 m. The 1D Vs values for MASW 2 (Figure 9(a)) increases from 232 m/s to 473 m/s at a depth of 3 m and 24 m, respectively, but the Vs values decreases from 470 m/s to 420 m/s at a depth of 24.5 m and 30 m, respectively. The 2D Vs cross-section for MASW 2 (Figure 9(b)) showed variations in Vs values across a distance of 115 m in which Vs values is being increased from 260 m/s to 382 m/s at a depth of 0 and 5 m, respectively, reducing at a depth of 10 m and increased in Vs at a depth of 13 m. Vs increased from 228 m/s at the surface to 406 m/s at a depth of 24.2 m, then dropped from 400 m/s to 200 m/s at a depth of 30 m as can be seen from 1D Vs profile from MASW 3 (Figure 10(a)). The 2D Vs cross-section of MASW 3 (Figure 10(b)) showed a change in Vs over a distance of 120 m along the survey line. The Vs increasing from 206 m/s to 294 m/s at a depth of 0 and 10 m, respectively, over a distance of 0 to 45 m but low Vs zone showed over a distance of 45 m to 120 m at a depth of 15 m.

At MASW 4, Vs ranges from 223 m/s to 300 m/s (Figure 11(a)). As compared to the other sites, MASW 4

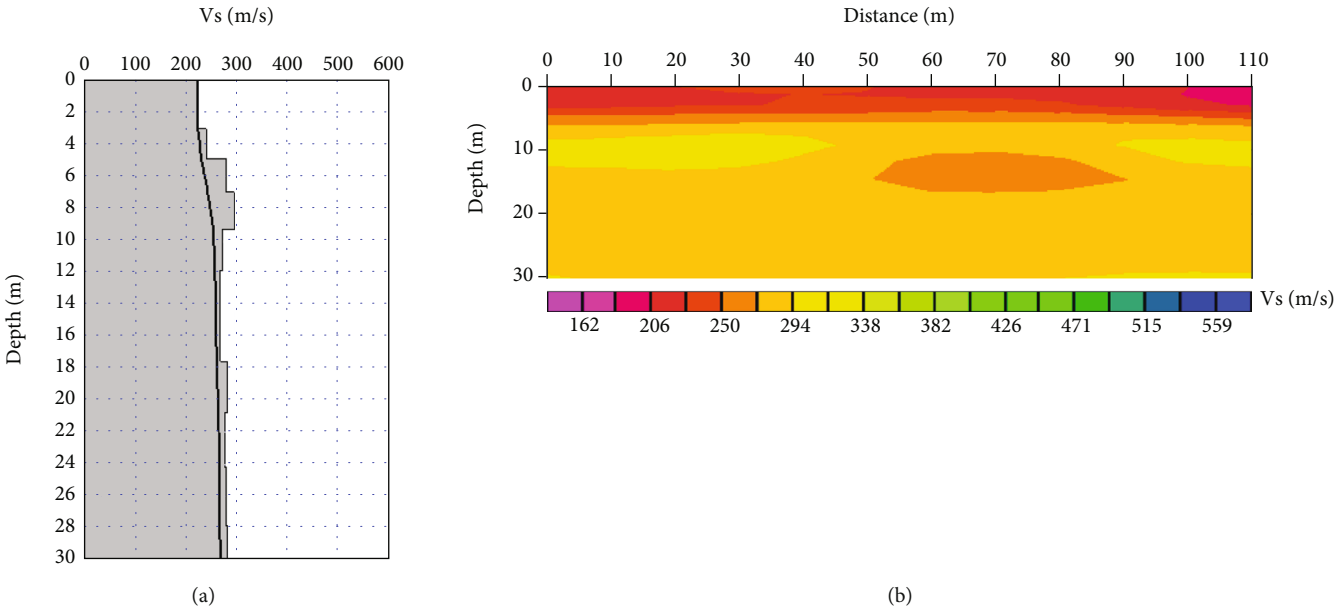

Figure 11: (a) MASW 4 1D Vs profile and (b) MASW 4 2D Vs cross-section.

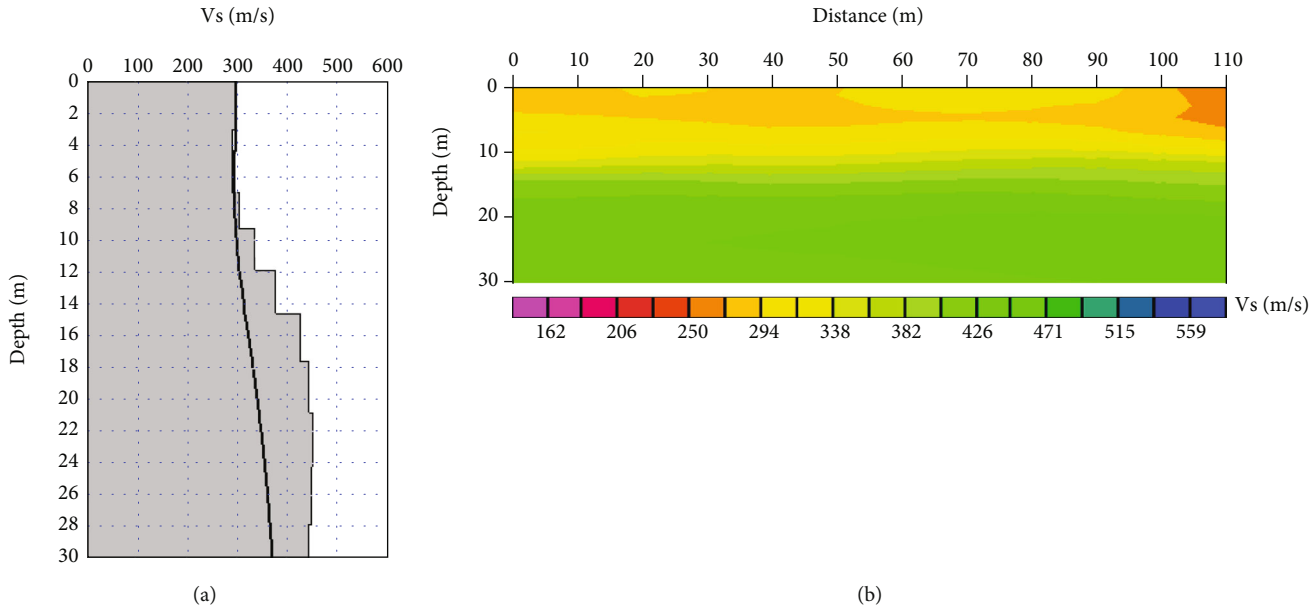

Figure 12: (a) MASW 5 1D Vs profile and (b) MASW 5 2D Vs cross-section.

showed a small increment in Vs with depth in which Vs reached a maximum of 300 m/s. The 2D Vs cross-section of MASW 4 showed a spatial variation over a distance of 110 m (Figure 11(b)) with a general increase in Vs with depth in which a low Vs ranging from 206 m/s to 272 m/s near to the surface to a depth of 7 m and a higher Vs which is greater than 292 m/s showed at a depths of 30 m. Moreover, for MASW 5 Vs values range from 300 m/s to 450 m/s at the surface to a depth of 30 m (Figure 12(a)). The Vs was found to decrease from 300 m/s at the surface to 450 m/s at a depth of 24 m but showed slight decrease in the Vs at a depth of 27.8 m. The 2D Vs cross-section has shown for MASW 5 the variation of Vs values across a distance of 110 m (Figure 12(b)). The Vs increased from 272 m/s (at the surface) to 471 m/s at a depth of 30 m. Finally, 2D Vs cross-section revealed Vs values of 426 m/s for depths ranging from 16 m to 30 m over a distance of 0 to 110 m.

6.3. Vs30, G30max, and E30 Map. The Vs30 data from several sites were collected and used to create a Vs30 map for Hawassa town. The Vs30 values for Hawassa town range from 248.9 m/s to 371.3 m/s as can be seen from

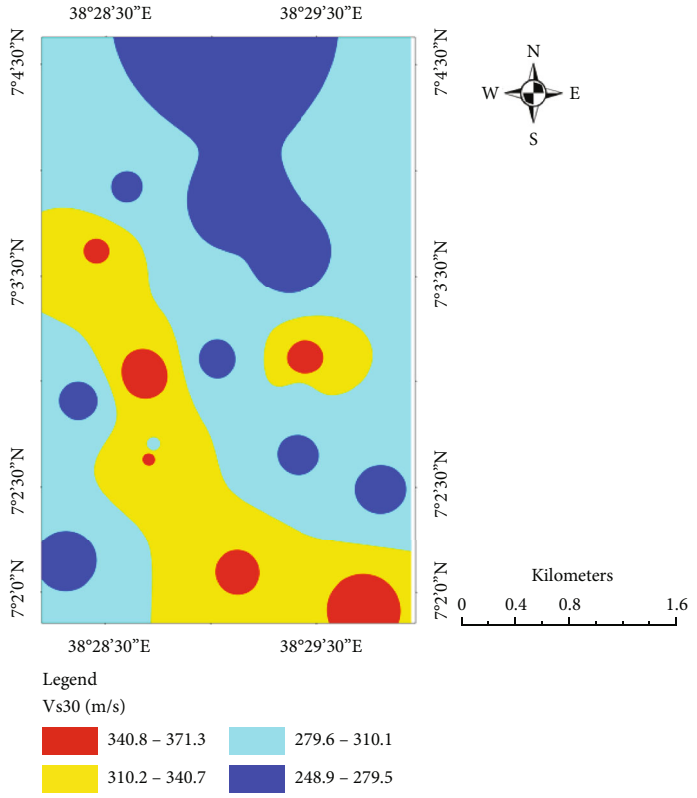

(a)

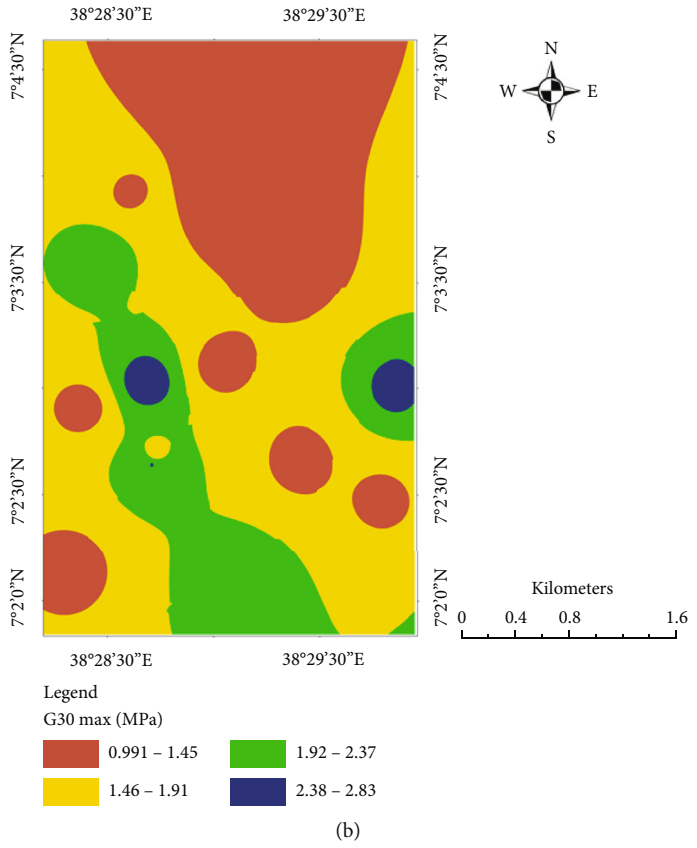

(b)

Figure 13: Continued.

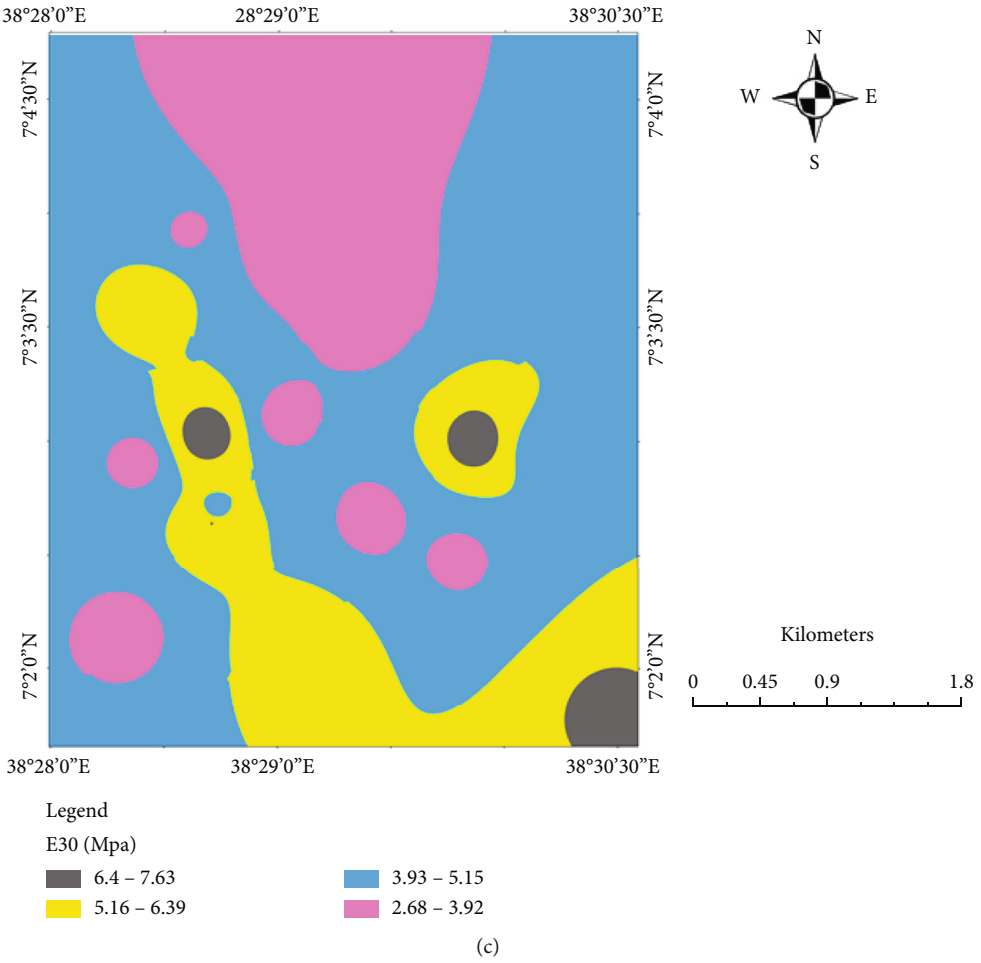

(c)

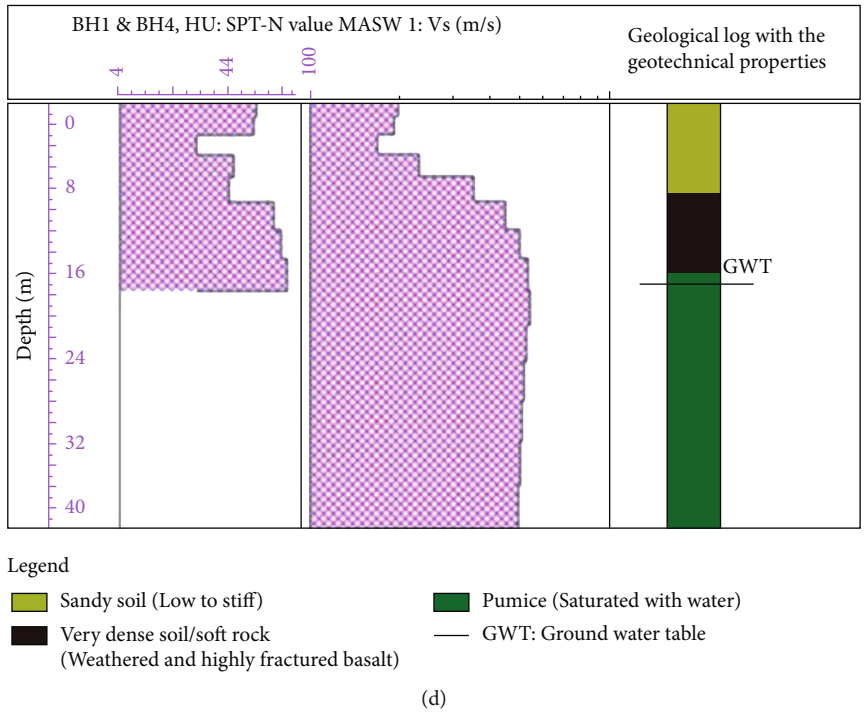

(d)

Figure 13: (a) Vs30 map of Hawassa town, (b) Gmax30 map of Hawassa town, (c) E30 map of Hawassa town, and (d) Lithological correlation between SPTN Values (BH1, BH4, and HU) with Vs for MASW 1.

Figure 13(a). A very low Vs30 values, which range from 248.9 m/s m/s to 279.5 m/s, were found in the northern and to some extent in central parts of the study area while the low Vs30 values, which range from 279.6 m/s to 310.1 m/s, were found in the eastern, some parts of the western, and central areas. A high Vs30 values, ranging from 310.2 m/s to 340.7 m/s were found in the western, southern, and some central parts of the study area. In the southern as well as some sites in the western and eastern parts of the study area, very high Vs30 values, ranging from 340.5 m/s to 371.3 m/s, were found. Hence, the study area (Table 5) falls under C and D site classes according to [72] but classes B and C according to [73]. When Vs30 values were correlated to [72] soil classes, the majority of the soils in the study area were classified as stiff soils with a minor portion of very stiff soil or soft rock but the study area is mostly covered with medium dense sand and very dense sand according to [73].

The G30max and E30 maps were generated to characterize Hawassa town. The near-subsurface materials up to the depth 30 m were mapped using G30max values which vary from 0.991 MPa to 2.83 MPa in this investigation. The G30max map (Figure 13(b)) revealed the presence of (a) high stiff materials in the southern, southeastern, and southwestern corridors and (b) very low stiff materials in the northern, western, and central parts of the study area. Due to its lower stiffness, the northern part of the study area requires more attention in terms of its engineering design attention than the southern portion of the study area, which has a higher stiffness. The E30 map was prepared to characterize the degree of deformation in earth materials for settlement studies in the study area. The E30 map showed that the E30 values range from 2.68 MPa to 7.63 MPa. This map (Figure 13(c)) revealed that the northern and central parts of the study area have a lower modulus of elasticity, indicating a higher deformation whereas the southern part has got a higher modulus of elasticity, implying a smaller deformation. This means that in the northern portion of the study area, settlement analysis is required more than that of the southern part. The lithological correlation between SPT-N borehole, Vs and borehole log (BH1 and BH4: HU) were done for MASW 1 to understand the vertical stratification of the study area (Figure 13(d)). It was showed that a decrease in Vs and SPT-N values at a depth of 0 to 6 m and increases at a depth of 6 m to 18 m due to the presence of very dense soil and soft rocks (weathered and highly fractured basalt).

6.4. Geotechnical Soil Characterization. Grain size analysis for representative soil samples from the study area was conducted using sieve analysis. The grain size distribution ranges from 0% to 5% for gravel, 25% to 89% for sand and 11% to 80% for nonplastic silt in the study area (Figure 14(a)). Hence, the Atterberg limits were not determined or not possible (NP) to determine for the representative soils in the study area as it is dominated by nonplastic cohessionless soils (Table 6). The soils in the study area soil were dominantly silty sand and sand according to the Unified Soil Classification System (USCS). The result of the current study is similar with that of [71].

Table 5: Vs30 values of the respective site classes in Hawassa town.

Site codes	Vs30 (m/s)	Site classes of Hawassa town	
		According to [72]	According to [73]
MASW 1	362	C	B
MASW 2	350	D	C
MASW 3	301	D	C
MASW 4	269	D	C
MASW 5	371	C	B
MASW 6	301	D	C
MASW 7	346	D	C
MASW 8	266	D	C
MASW 9	261	D	C
MASW 10	268	D	C
MASW 11	271	D	C
MASW 12	276	D	C
MASW 13	356	D	C
MASW 14	357	D	C
MASW 15	270	D	C
MASW 16	348	D	C
MASW 17	267	D	C
MASW 18	265	D	C
MASW 19	249	D	C

6.5. Correlation of Vs between SPT-N and N60. For the regression correlation of Vs and SPT-N values using the power law, data pairs of Vs, and SPT-N were used. The relationship between Vs and SPT-N values was investigated using a linear regression approach. Attempts were made in this work to derive Vs from SPT-N and N60 data for Hawassa town (Supplementary Table S3). The geology of the study area is characterized by sandy soil to according to SPT-N values, well inventory, and MASW data. As a result, for the study area with a similar soil types, different empirical equations were compared to the newly developed Vs using SPT-N and N60 regression equations. Figure 15(a) depicts the linear regression equation derived in this study as well as other equations developed for similar soil characteristics (i.e. sandy soil). The SPT-N value has a considerable effect on Vs estimate as evidenced by the high Pearson correlation coefficient (R^2). The proposed correlation between Vs and SPT-N values for Hawassa town is given in equation (7) as follows.

$$V_s = 115(\mathrm{SPT} - N)^{0.28} \left(r = 0.84 \text{ and } R^2 = 0.7102 \text{ for sandy soil}\right). \quad (7)$$

The correlation model was made using the power law (equation (8)) and the Vs and N60 proposed equations for the town of Hawassa (Figure 10(a)).

$$V_s = 122.98N60^{0.2807} \left(r = 0.714 \text{ and } R^2 = 0.5102 \text{ for sandy soil}\right). \quad (8)$$

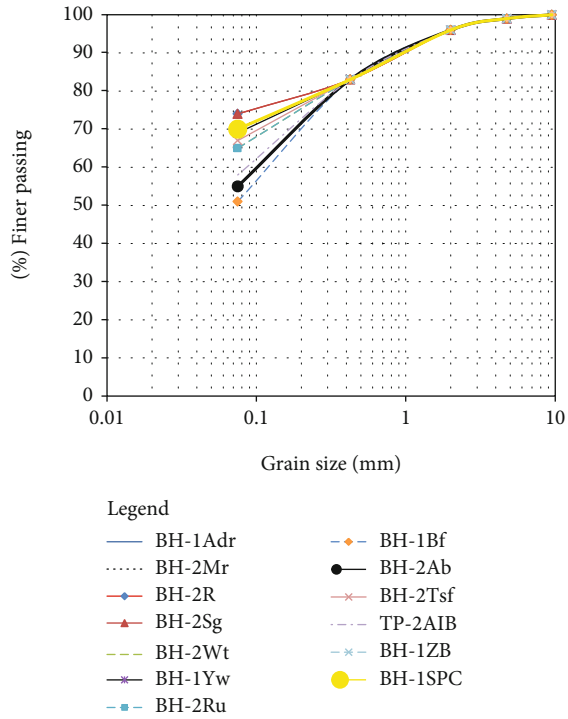

Figure 14: Grain size distribution curves of soil in the study area.

Table 6: Summarized geotechnical results of soils in the study area.

Borehole and pit code	Depth (m)	Atterberg limit			%			USCS	
		LL	PL	PI	Gravel	Sand	Fine		
BH-1Adr	3	NP	NP	NP	—	25	75	Silty sand soil	SM
BH-1HU	3	NP	NP	NP	—	95	5	Poorly graded sand soil	SP
BH-2Mr	3	NP	NP	NP	—	20	80	Silty sand soil	SM
BH-2R	3	NP	NP	NP	5	25	70	Silty sand with some gravel soil	SM
BH-2Ru	3	NP	NP	NP	—	38	62	Silty sand soil	
BH-2Sg	3	NP	NP	NP	—	33	67	Silty sand soil	
BH-2Wt	3	NP	NP	NP	—	45	55	Silty sand soil	
BH-1Yw	3	NP	NP	NP	—	50	50	Silty sand soil	
BH-2Ab	3	NP	NP	NP	—	40	60	Silty sand soil	
BH-1Bh	3	NP	NP	NP	—	44	56	Silty sand soil	SM
BH-2Tsf	3	NP	NP	NP	—	41	59	Silty sand soil	
TP-2AIB	3	NP	NP	NP	—	39	61	Silty sand soil	
BH-1SPC	3	NP	NP	NP	—	25	75	Silty sand soil	
BH-1ZB	3	NP	NP	NP	—	34	66	Silty sand soil	
PIT1	2	NP	NP	NP	—	32	68	Silty sand soil	

As stated in equations (7) and (8), strong relation from R^2 were found for Vs and SPT-N values rather than the Vs and N60 values in this investigation. In general, an equation with a high R^2 value can predict more accurately than the one with a lower value. Hence, the results showed that the predicting equation based on SPT-N values (equation (7)) has a more predictive capacity to forecast Vs than N60 in this study (equation (8)). Furthermore, the suggested Hawassa town linear regression model was tested using Cd and a comparison of Vspred and Vsmeas. Figure 15(b) shows a comparison of Cd and SPT-N levels for sandy soils in the study area. It should be noticed that Cd's average value was close to zero (Supplementary Table S4 and Figure S3). This

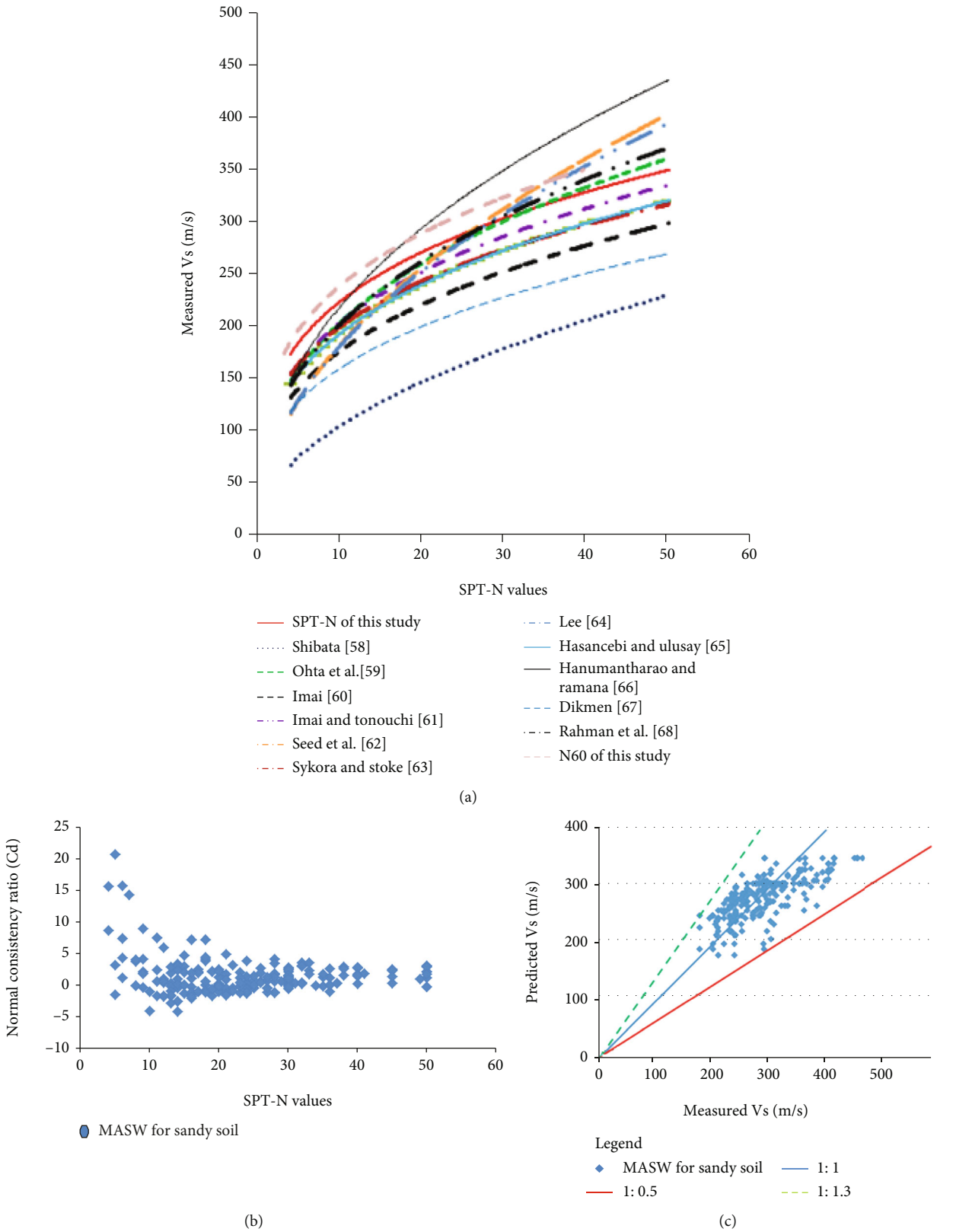

Figure 15: (a) correlations between Vs, SPT-N and N60 of the current and previous studies, (b) Cd graphs of sandy soil, and (c) comparison between predicted and measured Vs for sandy soil.

means that the predicted Vs value is quite close to the measured one. As a result, the Cd ratio validation test for the newly proposed regression equation developed for the study area estimates Vs accurately and confidently. In addition, comparisons between Vsmeas and Vspred were done. Figure 15(c) depicts the Vsmeas and Vspred for the validation of the newly proposed regression equation for Hawassa town. All of the data points fall between the 1 : 0.5 and 1 : 1.3 slope lines. However, majority of the data fall inside the 1 : 1 line slope indicating that the predictive model is the best fit for study the area (Supplementary Table S5 and Figure S4).

7. Conclusions

The VES and borehole data indicated that a groundwater table is found at shallow depth in the study area. The Vs values for Hawassa town from a 1D profile range from 191 m/s to 542 m/s whereas the Vs30 values ranges from 248.9 m/s to 371.3 m/s. The 2D Vs cross-section has shown the low velocity layer at a shallow depth that need good engineering design. SPT-N values in the study area range from 5bpf to 50bpf. The SPT-N values showed sandy soil with low to medium stiffness at a shallow depth. According to the Natural Earthquake Hazard Reduction Program (NEHRP) classification methodology, the near-surface materials in Hawassa town are classified as site classes C and D but according to the Eurocode (EC8) protocols, they are classified as site classes B and C. Therefore, the seismic design for site class D in the study area is required to minimize the earthquake hazards. The near-surface materials in Hawassa town have Gmax30 values ranging from 0.991 MPa to 2.83 MPa, and E30m values ranging from 2.68 MPa to 7.63 MPa. The produced Vs30, Gmax30, and E30 maps showed low values in the northern part and high values in the southern part of the study area. Therefore, the northern part needs more attention with respect to engineering design than the southern part of the study area. The results of Cd, R^2, and comparison of Vspred and Vsmeas showed that the newly proposed regression equation can be effectively used to determine Vs for engineering site characterization in areas with similar geological ad geotechnical conditions in Ethiopia and elsewhere in the world if there is limited budget and time. The grain size analysis showed that the soils in the study area are silty sand and sand soil. For full subsurface characterization in the study area, 3D Vs modeling and microtremor surveys are needed. The findings of this study can be used as first-hand information for future seismic hazard evaluation and site response analysis in Hawassa town and its environs.

Data Availability

Some of data analyzed during this study are included in this manuscript. In addition, the remaining datasets used for this study are available with the corresponding author which can be provided based on a reasonable request.

Conflicts of Interest

The authors have declared that there is no conflict of interest with any individual, company or organization regarding the publication of this work.

Authors' Contributions

The first author has done the data collection, analysis and draft write up of the manuscript. The second and third authors commented and enriched the manuscript in each phase and all authors read and approved the final manuscript.

Acknowledgments

The first author also would like to thank Wachemo University and Addis Ababa Science and Technology University for the financial support.

Supplementary Materials

The authors provided the borehole, SPT-N, N60, Vs and Vp data, and their representations in the graphs in the supplementary file. *(Supplementary Materials)*

References

[1] S. Rahimi, C. M. Wood, P. Kokkali, and B. Rivers, "Advantages of geophysics to improve site characterization and reliability for transportation projects," *Transportation Research Record*, vol. 2675, no. 7, pp. 540–554, 2021.

[2] W. J. Stephenson, A. Yong, and A. Martin, "Flexible multimethod approach for seismic site characterization," *Journal of Seismology*, vol. 26, no. 4, pp. 687–711, 2022.

[3] A. Ayele, K. Woldearegay, and M. Meten, "A review on the multi-criteria seismic hazard analysis of Ethiopia: with implications of infrastructural development," *Geoenvironmental Disasters*, vol. 8, no. 1, pp. 1–22, 2021.

[4] O. Ademila, "Pre-foundation geophysical investigation of a site for structural development in Oka, Nigeria," *NRIAG Journal of Astronomy and Geophysics*, vol. 11, no. 1, pp. 81–112, 2022.

[5] D. Chandran and P. Anbazhagan, "2D nonlinear site response analysis of typical stiff and soft soil sites at shallow bedrock region with low to medium seismicity," *Journal of Applied Geophysics*, vol. 179, article 104087, 2020.

[6] O. Ademila, "Combined geophysical and geotechnical investigation of pavement failure for sustainable construction of Owo-Ikare highway, Southwestern Nigeria," *NRIAG Journal of Astronomy and Geophysics*, vol. 10, no. 1, pp. 183–201, 2021.

[7] A. O. Oladotun, J. E. Oluwagbemi, A. M. Lola, O. Maxwell, and A. Sayo, "Predicting dynamic geotechnical parameters in near-surface coastal environment," *Cogent Engineering*, vol. 6, no. 1, pp. 1–11, 2019.

[8] K. D. Oyeyemi, O. M. Olofinnade, A. P. Aizebeokhai et al., "Geoengineering site characterization for foundation integrity assessment," *Cogent Engineering*, vol. 7, no. 1, pp. 1–15, 2020.

[9] E. Ausilio, M. G. Durante, and P. Zimmaro, "Best practices for developing geotechnical models and seismic hazard

procedures for critical infrastructure: the viadotto Italia case study in Southern Italy," *Geosciences*, vol. 12, no. 8, p. 295, 2022.

[10] O. Igwe and A. A. Umbugadu, "Characterization of structural failures founded on soils in Panyam and some parts of Mangu, Central Nigeria," *Geoenvironmental Disasters*, vol. 7, no. 1, pp. 1–26, 2020.

[11] D. M. Naji, M. K. Akin, and A. F. Cabalar, "A comparative study on the V_{S30} and N_{30} based seismic site classification in Kahramanmaras, Turkey," *Advances in Civil Engineering*, vol. 2020, Article ID 8862827, 15 pages, 2020.

[12] N. Ferguson and G. Gautreau, *Feasibility Study on Geophysical Methods to Estimate Geotechnical Properties in Louisiana (No. FHWA/LA. 22/667)*, Department of Transportation and Development, Louisiana, 2022.

[13] H. Jusoh, S. B. S. Osman, and K. A. M. Noh, "Usability of the surface wave method in assessment for subsurface investigation," *IOP Conference Series: Earth and Environmental Science*, vol. 1003, no. 1, article 012039, 2022.

[14] A. Rubaiyn, A. Priyono, and T. Yudistira, "Near -surface S-wave estimation based on inversion of Rayleigh wave dispersion curve using genetic algorithm," *IOP Conference Series: Earth and Environmental Science*, vol. 318, no. 1, pp. 12-13, 2019.

[15] N. Le Ngal, S. Pramumijoyo, I. Satyarno, K. S. Brotopuspito, J. Kiyono, and E. Hartantyo, "Multi-channel analysis of surface wave method for geotechnical site characterization in Yogyakarta, Indonesia," *E3S Web of Conferences*, vol. 76, article 03006, 2019.

[16] K. S. Ishola, B. D. Amu, and L. Adeoti, "Evaluation of near-surface conditions for engineering site characterization using geophysical and geotechnical methods in Lagos, Southwestern Nigeria," *NRIAG Journal of Astronomy and Geophysics*, vol. 11, no. 1, pp. 237–256, 2022.

[17] G. Cultrera, C. Cornou, G. Di Giulio, and P. Y. Bard, "Indicators for site characterization at seismic station: recommendation from a dedicated survey," *Bulletin of Earthquake Engineering*, vol. 19, no. 11, pp. 4171–4195, 2021.

[18] G. Wang, H. Wang, H. Li, Z. Lu, W. Li, and T. Xu, "Application of active-source surface waves in urban underground space detection: a case study of Rongcheng County, Hebei, China," *Earth and Planetary Physics*, vol. 6, 2022.

[19] R. Arjwech and M. E. Everett, "Electrical resistivity tomography at construction sites in northeast Thailand with implications for building foundation design," *Journal of Environmental and Engineering Geophysics*, vol. 24, no. 2, pp. 333–340, 2019.

[20] S. Wahab, H. Saibi, and H. Mizunaga, "Groundwater aquifer detection using the electrical resistivity method at Ito Campus, Kyushu University (Fukuoka, Japan)," *Geoscience Letters*, vol. 8, no. 1, pp. 1–8, 2021.

[21] Z. Guan and Y. Wang, "Selection of standard penetration test number for geotechnical investigation of a vertical cross section considering spatial variability and correlation in soil properties," *Canadian Geotechnical Journal*, vol. 58, no. 11, pp. 1654–1668, 2021.

[22] M. Ghali, M. Chekired, and M. Karray, "Framework to improve the correlation of SPT-N and geotechnical parameters in sand," *Acta Geotechnica*, vol. 15, no. 3, pp. 735–759, 2022.

[23] M. R. Motahari, O. Amini, A. Khoshghalb, M. Etemadifar, and N. Alali, "Investigation of the geotechnical properties and estimation of the relative density from the standard penetration test in sandy soils (case study: north east of Iran)," *Geotechnical and Geological Engineering*, vol. 40, no. 5, pp. 2425–2442, 2022.

[24] C. G. Sun, H. I. Cho, H. S. Kim, and M. G. Lee, "Determining N value from SPT blows for 30 cm penetration in weathered strata," *Geomechanics and Engineering*, vol. 28, no. 6, pp. 625–636, 2022.

[25] K. Bajaj and P. Anbazhagan, "Seismic site classification and correlation between V_S and SPT-N for deep soil sites in Indo-Gangetic Basin," *Journal of Applied Geophysics*, vol. 163, pp. 55–72, 2019.

[26] M. B. Hossain, M. M. Rahman, and M. R. Haque, "Empirical correlation between shear wave velocity (Vs) and uncorrected standard penetration resistance (SPT-N) for Dinajpur District, Bangladesh," *Journal of Nature*, vol. 3, pp. 25–29, 2021.

[27] W. Duan, G. Cai, S. Liu, and A. J. Puppala, "Correlations between shear wave velocity and geotechnical parameters for Jiangsu clays of China," *Pure and Applied Geophysics*, vol. 176, no. 2, pp. 669–684, 2019.

[28] A. Kumar, R. Satyannarayana, and B. G. Rajesh, "Correlation between SPT-N and shear wave velocity (V_S) and seismic site classification for Amaravati city, India," *Journal of Applied Geophysics*, vol. 205, article 104757, 2022.

[29] S. Atsbahaa, H. Gebrub, T. Haileb, and A. Legessec, "Joint application of geophysical techniques for engineering site characterization of Samara University Area, Ethiopia," *Journal of Geology & Geophysics*, vol. 8, no. 467, pp. 10–35248, 2019.

[30] P. Anbazhagan, K. Ayush, M. E. Yadhunandan, K. Siriwanth, K. Suryanarayana, and G. Sahodar, "Effective use of SPT: hammer energy measurement and integrated subsurface investigation," *Indian Geotechnical Journal*, vol. 52, no. 5, pp. 1079–1096, 2022.

[31] D. Maestrelli, G. Corti, M. Bonini, D. Montanari, and F. Sani, "Caldera collapse and tectonics along the main Ethiopian rift: reviewing possible relationships," *Comptes Rendus Géoscience*, vol. 353, no. S2, pp. 1–19, 2021.

[32] A. Lavayssière, T. Greenfield, D. Keir, A. Ayele, and J. M. Kendall, "Local seismicity near the actively deforming Corbetti volcano in the Main Ethiopian Rift," *Journal of Volcanology and Geothermal Research*, vol. 381, pp. 227–237, 2019.

[33] G. Berhanu, "Geology, petrology and geochemistry of volcanic rocks around Arba Minch, Southern Ethiopia," *Earth*, vol. 8, no. 3, pp. 160–168, 2019.

[34] G. Corti, F. Sani, A. A. Florio et al., "Tectonics of the Asela-Langano margin, Main Ethiopian Rift (East Africa)," *Tectonics*, vol. 39, no. 8, article e2020TC006075, 2020.

[35] B. Kebede, T. Mammo, and A. Misgie, "Structural interpretation of Southern Main Ethiopian Rift basin using constrained full tensor gravity inversion of the basement morphology," *Heliyon*, vol. 8, no. 5, article e09525, 2022.

[36] V. Ţáček, V. Rapprich, Y. Aman et al., *Explanation booklet to the set of geosciences map of Ethiopia at a scale 1: 50,000*, Geological Survey of Ethiopia, 2014.

[37] A. P. Panjamani and S. G. Ingale, "Status quo of standard penetration test in India: a review of field practices and suggestions to incorporate in Is 2131," *Indian Geotechnical Journal*, vol. 51, no. 2, pp. 421–434, 2021.

[38] X. Li, Y. Li, D. Lv, S. He, and W. Zhang, "Influence of drilling methods on results of standard penetration test in Loess–Paleosol sequence," *Frontiers in Built Environment*, vol. 8, article 846815, 2022.

[39] ADDIS GEOSYSTEM CO.LTD, *Geotechnical investigation report of Hawassa town, Southern Ethiopia*, ADDIS GEOSYSTEM CO.LTD, 2015.

[40] ARCON Design Build Plc, *Geotechnical investigation report of Hawassa town, Southern Ethiopia*, ARCON Design Build Plc, 2018.

[41] A. W. Skempton, "Standard penetration test procedures and the effects in sands of overburden pressure, relative density, particle size, ageing and overconsolidation," *Geotechnique*, vol. 36, no. 3, pp. 425–447, 1986.

[42] D. P. Balasubramani and G. R. Dodagoudar, "Modelling the spatial variability of standard penetration test data for Chennai City using kriging and product-sum model," *Geomechanics and Geoengineering*, vol. 17, no. 1, pp. 92–105, 2022.

[43] ASTM D422-63, *Standard test method for particle-size analysis of soils*, ASTM International, West Conshohocken, 2007.

[44] South Design and Construction Supervision Enterprise (SDCSE), *Groundwater exploration water supply project draft report of Hawassa town, Southern Ethiopia*, South Design and Construction Supervision Enterprise (SDCSE), 2019.

[45] A. Bobatchev, I. Modin, and V. Shevnin, *IPI2WIN Resistivity Sounding Interpretation program*, Moscow State University, Moscow, Russia, 2001, Version 2.0, User's manual 15.

[46] V. D. Rao and D. Choudhury, "Estimation of shear wave velocity and seismic site characterization for new nuclear power plant region, India," *Natural Hazards Review*, vol. 21, no. 4, article 06020004, 2020.

[47] W. Wu, J. Liu, L. Guo, and Z. Deng, "Methodology and assessment of proxy-based Vs30 estimation in Sichuan Province, China," *International Journal of Disaster Risk Science*, vol. 11, no. 1, pp. 133–144, 2020.

[48] J. Wang and T. Tanimoto, "Estimation of Vs30 at the Earth scope transportable array stations by inversion of low-frequency seismic noise," *Journal of Geophysical Research: Solid Earth*, vol. 127, no. 4, article e2021JB023469, 2022.

[49] D. Steeples and R. D. Miller, "1. Seismic reflection methods applied to engineering, Environmental, and groundwater problems," *Geotechnical and Environmental Geophysics*, vol. 1, no. 5, pp. 1–30, 1990.

[50] B. Hasselström, "Water prospecting and rock-investigation by the seismic refraction method," *Geoexploration*, vol. 7, no. 2, pp. 113–132, 1969.

[51] S. Fukushima, M. Shinohara, K. Nishida, A. Takeo, T. Yamada, and K. Yomogida, "Detailed S-wave velocity structure of sediment and crust off Sanriku, Japan by a new analysis method for distributed acoustic sensing data using a seafloor cable and seismic interferometry," *Earth, Planets and Space*, vol. 74, no. 1, pp. 1–11, 2022.

[52] C. Kitsunezaki, "Estimation of P- and S-wave velocities in deep soil deposits for evaluating ground vibrations in earthquake," *Journal of the Japan Society for Natural Disaster Science*, vol. 9, pp. 1–17, 1990.

[53] R. Sarkar, S. Kolathayar, D. Drukpa et al., "Near-surface seismic refraction tomography and MASW for site characterization in Phuentsholing, Bhutan Himalaya," *SN Applied Sciences*, vol. 3, no. 4, pp. 1–18, 2021.

[54] J. Sharifi, M. Nooraiepour, M. Amiri, and N. H. Mondol, "Developing a relationship between static Young's modulus and seismic parameters," *Journal of Petroleum Exploration and Production Technology*, vol. 12, pp. 1–16, 2022.

[55] J. Reynolds, *An introduction to applied and environmental geophysics*, John Wiley and Sons Ltd, New York, 1997.

[56] P. Kearey, M. Brooks, and I. Hill, *An introduction to geophysical exploration*, Blackwell Science Ltd, UK, 3rd edition edition, 2002.

[57] M. Ashikuzzaman, A. Hossain, M. S. A. Salan, M. A. Rahman, and M. M. Hasan, "Development of empirical correlations between shear wave velocity and standard penetration value: a case study of Rajshahi District, Bangladesh," *American Journal of Mechanical and Industrial Engineering*, vol. 6, no. 1, pp. 1–6, 2021.

[58] T. Shibata, "Analysis of liquefaction of saturated sand during cyclic loading," *Disaster Prevention Res. Inst. Bull*, vol. 4, pp. 34–45, 1970.

[59] T. Ohta, A. Hara, M. Niwa, and T. Sakano, "Elastic shear moduli as estimated from N-value," in *The proceeding 7th Annual Convention of Japan Society of Soil Mechanics and Foundation Engineering*, pp. 265–268, Japan, 1972.

[60] T. Imai, "P-and S-wave velocities of the ground in Japan," *The Proceedings of 9th International Conference on Soil Mechanics and Foundation Engineering*, vol. 2, pp. 127–132, 1977.

[61] T. Imai and K. Tonouchi, "Correlation of N value with S-wave velocity and shear modulus," in *The proceeding of 2nd European Symposium on penetration testing*, pp. 67–72, Amsterdam, 1982.

[62] H. B. Seed, I. M. Idriss, and I. Arango, "Evaluation of liquefaction potential using field performance data," *Journal of Geotechnical Engineering*, vol. 109, no. 3, pp. 458–482, 1983.

[63] D. E. Sykora and K. H. Stokoe, "Correlations of in-situ measurements in sands of shear wave velocity," *Soil Dynamics and Earthquake Engineering*, vol. 20, pp. 125–136, 1983.

[64] S. H. H. Lee, "Regression models of shear wave velocities in Taipei basin," *Journal of the Chinese Institute of Engineers.*, vol. 13, no. 5, pp. 519–532, 1990.

[65] N. Hasançebi and R. Ulusay, "Empirical correlations between shear wave velocity and penetration resistance for ground shaking assessments," *Bulletin of Engineering Geology and the Environment*, vol. 66, no. 2, pp. 203–213, 2007.

[66] C. Hanumantharao and G. V. Ramanan, "Dynamic soil properties for microzonation of Delhi, India," *Journal of Earth System Science*, vol. 117, no. S2, pp. 719–730, 2008.

[67] U. Dikmen, "Statistical correlations of shear wave velocity and penetration resistance for soils," *Journal of Geophysics and Engineering*, vol. 6, no. 1, pp. 61–72, 2009.

[68] M. Z. Rahman, *Probabilistic seismic hazard Analysis with nonlinear site response and liquefaction potential evaluation for deep sedimentary deposits, [Ph.D. thesis]*, University of British Columbia, 2019.

[69] D. Shukla and C. H. Solanki, "Estimated empirical correlations between shear wave velocity and SPT-N value for indore City using NLR and ANN," *Indian Geotechnical Journal*, vol. 50, no. 5, pp. 784–800, 2020.

[70] A. S. Daag, O. P. C. Halasan, A. A. T. Magnaye, R. N. Grutas, and R. U. Solidum Jr., "Empirical correlation between standard penetration resistance (SPT-N) and Shear Wave Velocity (Vs) for soils in Metro Manila, Philippines," *Applied Sciences*, vol. 12, no. 16, p. 8067, 2022.

[71] B. E. Alemu, A. Worku, G. M. Wassie, and G. T. Habtesellasie, "Ground response analysis of representative sites of Hawassa city," in *Geotechnical earthquake engineering and soil dynamics V: Seismic hazard analysis, earthquake ground motions, and regional-scale assessment*, pp. 422–434, American Society of Civil Engineers, Reston, VA, 2018.

[72] BSSC, *2015 Edition NEHRP recommended Seismic Provisions for New Buildings and Other Structures*, FEMA P-1050-1 (Provisions and Commentary), Washington, D.C., 2015.

[73] Eurocode-8, *BS-EN 1998-1, Design of structures for earthquake resistance part 1: General rules, seismic actions and rules for buildings*, European Committee for Standardization, Brussels, 2003.